Using Waveform Cross Correlation for Detection, Location, and Identification of Aftershocks of the 2017 Nuclear Explosion at the North Korea Test Site

by David P. Schaff, Won-Young Kim, Paul G. Richards, Eunyoung Jo, and Yonggyu Ryoo

ABSTRACT

We analyze a sequence of aftershocks of the 2017 nuclear explosion at the North Korea test site. Cross correlation is a powerful tool that takes advantage of waveform similarity to improve detection and location by 1–2 orders of magnitude as compared to analyzing events one-at-a-time. It can also help identify event type because if an event correlates well with another of known type, then it is likely of the same type. For a cluster of 13 aftershocks, we are able to achieve location estimates with high precision: the means of the 95% confidence ellipse semimajor and semiminor axes are only 69 and 19 m. The standard deviation of the residuals is only 0.0089 s, which is subsample and explains the residuals 171× better than our starting locations. We are able to image a fault 700 m long and conclude from correlation and location data that these events are all earthquakes. Complementary and independent analysis using *P*/*S* spectral ratios measured at only one station initially classified 12 of the events as earthquakes and 1 as an explosion, but the latter event appears to be a misclassification due to noise at one station. That one event appears to be earthquake-like even at that station, based on the similarity of the *Lg* waves with other events. The statistical significance of our results increases substantially combining our discriminant, correlation, and location data. We conclude that these events comprise an aligned cluster of small earthquakes, with a near-zero probability of misclassification.

Electronic Supplement: Map of area and stations used, group velocity plot of seismograms, and tables of correlation values.

INTRODUCTION

Correctly characterizing small magnitude seismic events ($\mathbf{M} < 3$) near nuclear test sites entails the challenging steps of detection, location, and identification. This work is important as part of the overall effort to drive downward the size of any test explosion that could with confidence (on the side that carried out the explosion) be undetected or unidentified. The capability to monitor even for small-yield explosions has the potential to give information on the sophistication of a nuclear weapons program (according to Chidambaran, 2000, it is harder to make a subkiloton device than a large-yield one); and we may also note that even a nuclear test explosion that misperforms and gives a low yield can potentially be revealed.

The North Korea test site appears to be the only place, so far, where nuclear test explosions have been conducted since 1998. There have also been several small seismic events near the test site, three of which were thought, at least initially by some researchers, to be small explosions and which have caused some concern.

The first was associated with a claim of De Geer (2012) for a low-yield nuclear explosion in Spring 2010, based on the detection of radionuclides near North Korea. Schaff *et al.* (2012) attempted to detect seismic signals from small explosions in North Korea for the five days in April and May 2010 proposed by De Geer (2012) but did not find evidence for a seismic event within the detection limits. Subsequent papers modeling the atmospheric transport of radionuclides focused on 11 May 2010 as the likely date of a claimed low-yield nuclear test in North Korea (De Geer, 2013; Wright, 2013). Zhang and Wen (2015) were able to successfully detect a very small seismic event ($\mathbf{M} \sim 1.5$) early on 12 May 2010 that they characterized unambiguously as a small nuclear explosion. This exceedingly small seismic event was not detected by the International Monitoring System, but Kim *et al.* (2017) found confirming evidence for it, concluding, even using data from Zhang and Wen (2015), that its signals were earthquake-like for frequencies between 6 and 12 Hz.

doi: 10.1785/0220180132

Some reports initially misclassified a second seismic event that occurred at 08:29 UTC on 23 September 2017 (**M** 3.3) among the aftershocks of the 2017 nuclear explosion. We provide evidence identifying this event as an earthquake.

A third seismic event among the aftershocks of the 2017 nuclear explosion was initially misclassified as an explosion at the North Korea test site in our companion paper in this issue (see fig. 6 of Kim *et al.*, 2018) and is discussed further in that paper. The event, the first of two to occur on 9 December 2017, was at first classified as an explosion using a linear discriminant based on three-component *P*/*S* spectral ratios at station MDJ alone. However, using a complementary and independent approach based on waveform cross correlation, we identify the event as an earthquake, with a near-zero probability of misclassification just from MDJ data, even though that data apparently include noise at a level which degrades spectral measurements. We refer to Kim *et al.* (2018) for a more complete discussion and summary of valid and understandable reasons why the discriminant method appeared to have misclassified the event due to a noise burst in the data. In that case, the method based on *P*/*S* spectral ratios was improved and gave what we believe to be the correct classification, via the addition of data from two more stations with lower signal-to-noise ratio (SNR) than MDJ.

Waveform cross correlation is a powerful tool that demonstrates 1–2 orders of magnitude improvement for many different applications. In this short article, we have simply applied the successful approach we have recently published in extensive detail for studies of thousands of seismic events in China (Schaff *et al*, 2018) to analyze aftershocks of North Korea's sixth nuclear test explosion. Our choices of seismic wave (*Lg*), frequency band, and time window, and our methods for measuring relative arrival times of neighboring events recorded at a common station and for characterizing the precision of our results, have all been guided by that previous experience.

DATA AND DETECTION

We first use a template event at station MDJ using a correlation detector to detect the aftershocks of the 2017 explosion. The detections worked well because these events have larger magnitudes (around 2.5–3.5), have similar magnitudes, are (as we shall further discuss) located within a few hundred meters of each other, and are of the same event type. In total, we analyzed 14 small seismic events at the North Korea test site. See Ⓔ Figure S1, available in the electronic supplement to this article for a map of the stations used. Eleven of these events were also reported by other agencies, and three were newly detected events. Details of the detection are described in our companion paper (Kim *et al.*, 2018).

LOCATION RESULTS

Absolute locations were obtained by manually picking *P* and *S* waves and using HYPOINVERSE (Klein, 2007) to locate the events (see Kim *et al.*, 2018 for details). Relative locations were obtained measuring differential travel times by waveform cross correlation for *Lg* waves. We followed the procedure described in Schaff *et al.* (2018) to make the correlation measurements and then solved for epicenters using a double-difference approach (Schaff and Richards, 2004). Out of the 14 starting events, we were able to locate 13 following this procedure. The starting locations are from Kim *et al.* (2018) and are reproduced in Ⓔ Table S1. Event 1, which is considered to be a cavity collapse that occurred 8.5 min after the 2017 explosion (Liu *et al.*, 2018; Tian *et al.*, 2018), was not located.

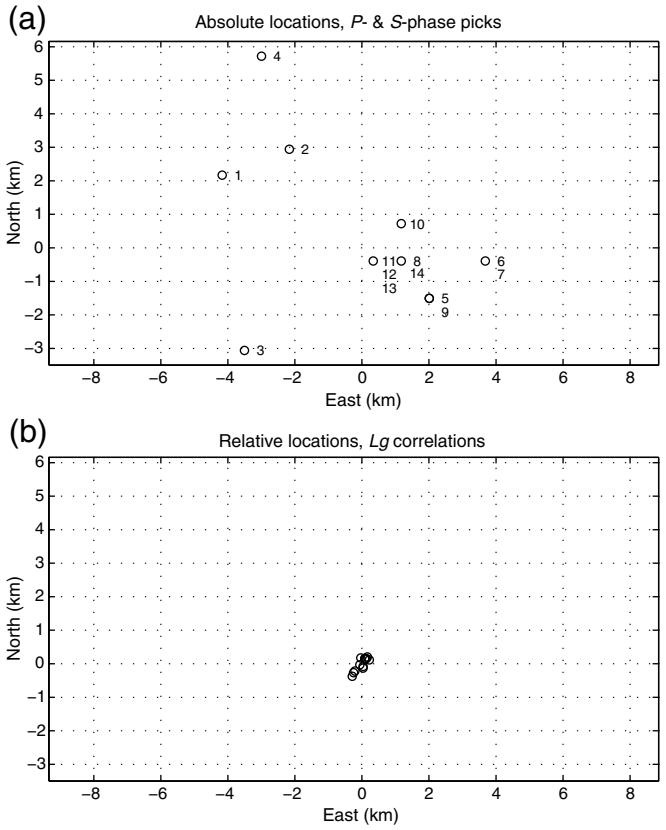

▲ **Figure 1.** (a) Absolute locations of a sequence of 14 events using *P*- and *S*-wave phase picks and (b) relative locations using *Lg* correlation data. Map axes are on the same scale.

Figure 1 compares the traditional absolute locations using *P*- and *S*-phase picks and a travel-time model with the relative locations using *Lg* cross-correlation measurements. There is significant improvement in the location precision of the relative locations as has been well established in the literature and as can be seen in the reduction in scatter. The standard deviation of the residuals of the *Lg* correlation measurements, using the absolute locations as a starting point, is 1.5176 s. The standard deviation of the *Lg* correlation measurements after relocation using the double-difference technique is 0.0089 s, which is a significant reduction (a factor of 171 improvement) in explaining the *Lg* residuals, being somewhat better even than what we were able to report for relocation of thousands of earthquakes in China (Schaff *et al.*, 2018). The median of the absolute value of the residuals is 0.0029 s. The highest sample rate of the data is 100 samples per second, so these

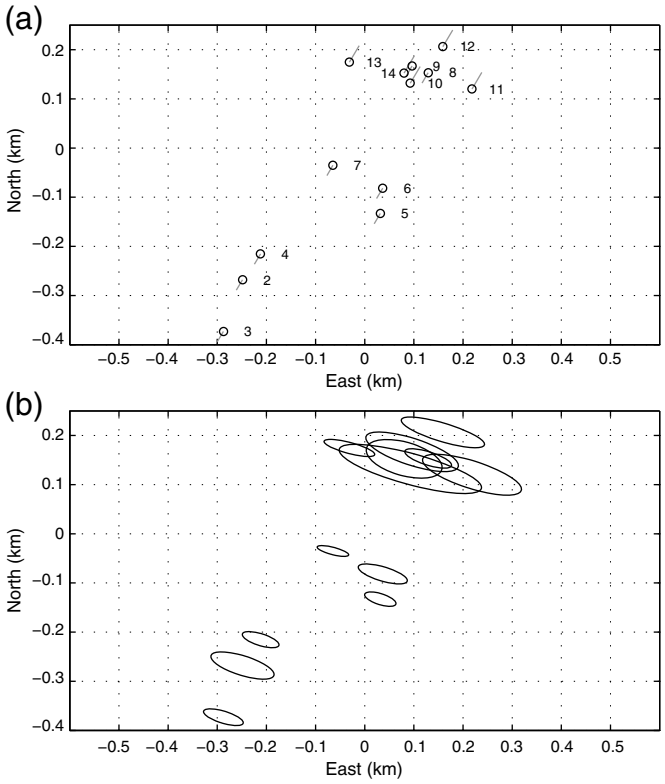

▲ **Figure 2.** (a) Zoomed-in plot of relative locations for 13 events. Circles show best locations based on initial locations starting at a point. End points of gray move vectors show locations perturbing initial locations by up to 1 km. (b) 95% confidence error ellipses for the 13 events in (a).

residuals of the correlation measurements indicate that subsample precision is achieved.

Figure 2 details the relative locations and error ellipses, zoomed in from Figure 1b. The 95% confidence formal error ellipses are small, the means of the semimajor and semiminor axes being only 69 and 19 m. The medians of the semimajor and semiminor axes are 53 and 15 m. In general support of such small numbers, we obtained independent empirical bootstrap-error estimates. The way the bootstrap-error ellipses are calculated makes them more sensitive to outliers, so we compare their median values of 80 and 19 m with the medians of the formal errors. We consider our location estimates for North Korea to be high quality, in terms of their fits to the residuals, error ellipses, and, in comparison, to locations previously obtained for thousands of events all over China and in nearby territories (Schaff *et al.*, 2018). Table 1 gives further details and comparisons with our previous work. The azimuthal gap in the present case is 153°, and the mean station distance is 410 km. Both of these are smaller than corresponding numbers (205°, 898 km) in our study of events all over China, which may be why our present results indicate even better precision.

The present set of aftershock events display the earthquake-like characteristic of being aligned as if on a fault about 700 m long and striking to the northeast (about 43°), which is well resolved because the length is in the direction of the semiminor axes of the error ellipses, with a mean of 13 m. The four pairs of doublet events that are observed to occur with recurrence intervals less than 6 hrs turn out to be exceptionally close to each other: 2 and 3, 6 and 7, 8 and 9, and 11 and 12. See Ⓔ Table S1, which gives our locations of these events and a discussion of the location quality.

Figures 3 and 4 display the aligned waveforms for all the events at station MDJ for the east component. It can be seen from the overlay of the waveforms at the bottom of each plot that they are very similar throughout most of the *Lg* wavetrain. It can also be seen that there is an evolution in the waveform shape as the events move from one end of the fault in Figure 2 to the other and that events that are located closer to each other have more-similar shape. The second arrival 23 s later after event 11 is event 12.

Ⓔ Table S2 shows the number of observations by event, as well as the mean, minimum, and maximum correlation coefficient (CC) values. About 8 out of the 13 events have a maximum CC value of 0.7 or greater with at least one other event, and 12 out of the 13 events have a maximum CC value

Table 1
Location Statistics for All of China, Wenchuan, and North Korea

	Number of Events Located	Mean *a* (km)	Mean *b* (km)	Median *a* (km)	Median *b* (km)	Move (km)	Gap (°)	Sigma res0 (s)	Sigma res (s)	MAD res (s)	Improve
All China	3689	0.42	0.09	0.37	0.07	0.04	205	3.7302	0.0417	0.0159	89×
Wenchuan	1934	0.37	0.08	0.35	0.07	0.05	266	0.8413	0.0267	0.0101	32×
North Korea	13	0.069	0.019	0.053	0.015	0.03	153	1.5176	0.0089	0.0029	171×

All China and Wenchuan, comparison of results from Schaff *et al.* (2018); North Korea, this study; *a*, semimajor axes of 95% confidence error ellipse; *b*, semiminor axes of 95% confidence error ellipse; Move, average shift in locations between two runs of starting at a point and perturbing initial locations by up to 1 km; Gap, azimuthal gap for cluster; sigma res0, standard deviation of correlation residuals at catalog locations; sigma res, standard deviation of correlation residuals after relocation; MAD res, median absolute deviation of correlation residuals after relocation; Improve, measure of improvement in relocation compared to catalog locations, sigma res0 divided by sigma res.

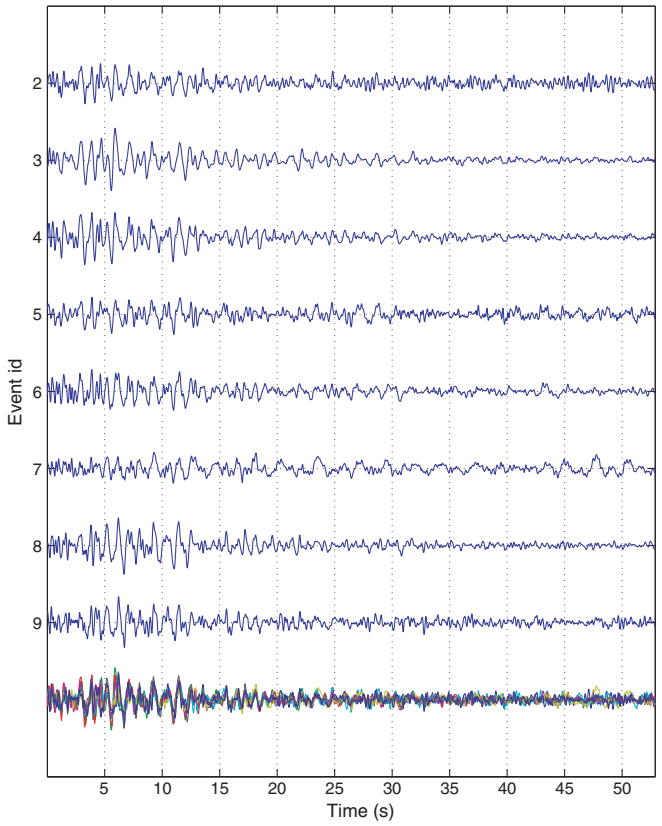

▲ **Figure 3.** Aligned waveforms at station MDJ on the east component for events 2–9. The bottom shows traces in different overlaying colors revealing high waveform similarity.

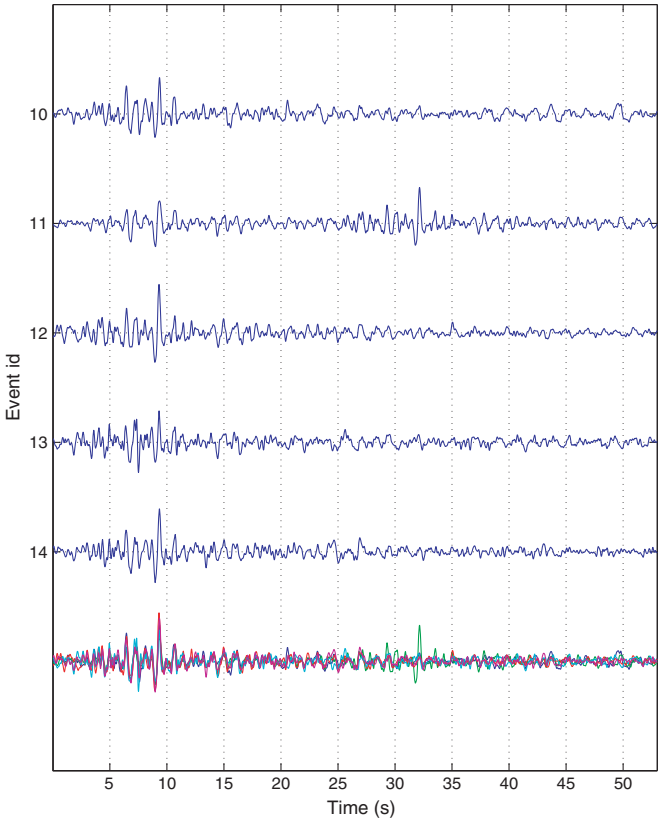

▲ **Figure 4.** Aligned waveforms at station MDJ on the east component for events 10–14. The bottom shows traces in different overlaying colors revealing high waveform similarity.

of 0.5 or greater with at least one other event. These are very high degrees of similarity and statistical significance for this time-bandwidth product (with 50 s windows and filtering from 0.5 to 5 Hz), which is why the differential travel-time measurements are such high quality with low residuals and error bars. For stations with lower CC values, this indicates that it is primarily due to lower SNR and not because the underlying waveforms are dissimilar. The mean CC value of the whole cluster is 0.43.

Ⓔ Figure S2 displays the observation matrix for the cluster of 13 events with the number of observations having CC ≥ 0.24 for each pair of events. This is important for determining how well connected the events are, both for constraining the locations and for identifying the cluster of events as a whole, as discussed later. The maximum CC values for the events also give confidence that each event belongs to the cluster. There is a total of 108 observations. All the differential travel-time measurements, CC values, and station coordinates are given in Ⓔ Tables S5 and S6 for other researchers interested in reproducing the results.

Ⓔ Figures S3 and S4 display the waveforms for 10 of the stations we used for the largest event in the cluster (the 23 September **M** 3.3, our event 3). Because we are using *Lg* correlation measurements, we must manage the fact that Ⓔ Figure S1 shows some of these paths crossing oceanic crust from the test site to stations in South Korea. In such cases, *Lg* does not propagate as efficiently and can be blocked entirely by a short oceanic path. See the Ⓔ electronic supplement for a discussion of how this affects our locations.

Our body-wave picks in Figure 1 have too great an uncertainty for reliable absolute locations for the position of this cluster, relative to the test site. But Tian *et al.* (2018) has good body-wave picks with low residuals and better data from stations in China, and they are able to get good relative locations between the 2017 explosion, cavity collapse, and our first three aftershocks (our events 2–4). Their locations for our events 2–4 are roughly located in a relative sense as our locations for the same events, showing agreement with different data and methods; the relative position they have for the three aftershocks relative to the 2017 explosion and cavity collapse places them about 7 km to the north and 1 km to the west of Mount Mantap, indicating that our candidate short fault may be several kilometers to the north.

INTERPRETATION AND IDENTIFICATION

The general subject of earthquakes induced by underground nuclear explosions has been described in some detail in the proceedings of a North Atlantic Treaty Organization (NATO)-sponsored conference held in Moscow in 1994 (Console

and Nikolaev, 1995). It includes papers by Adushkin and Spivak (1995) and Richards and Ekström (1995) that noted the occurrence of both low-frequency and high-frequency seismic aftershocks.

To interpret the locations of 13 high-frequency aftershocks of the 3 September 2017 underground nuclear explosion, we consider three possibilities: the events are earthquakes, explosions, or cavity collapses. Event 1, with the largest magnitude in the sequence, is the main cavity collapse. Its waveforms are not similar to those of the other 13 events. It has a mean CC of 0.12, whereas the cluster has a mean CC of 0.43 (see Ⓔ Table S2). If the 13 events were also cavity collapses close to event 1, we would expect their waveforms to be similar, but they are not, indicating that they are not nearby collapses. That is based on the similarity alone. Interpreting the locations of continued cavity collapses most likely would locate at a point or concentric circles with a small radius and not along a 700 m line.

We effectively rule out the possibility that these events are explosions from our linear discriminant that identifies 12 out of the 13 events to be earthquakes and not explosions (Kim *et al.*, 2018), with a near-zero probability of misclassifying all 12 events. More evidence that these events are not explosions is that the larger 23 September event (our event 3) is shown in Tian *et al.* (2018) to have polarity data that fit a double-couple source focal mechanism, and so they argue that it is an earthquake and not an explosion.

A third possibility is that these 13 events are earthquakes occurring on a fault with a strike that is well resolved in map view by our locations. The four sets of doublet events that occur close to each other, with similar magnitudes and within 6 hrs in each doublet, exhibit similar behavior to the short recurrence intervals of many of the repeating events identified in China by Schaff and Richards (2011). Independent evidence to support that this is an earthquake fault is that a focal mechanism for the orientation of the fault we image can fit the polarity data in Tian *et al.* (2018) within the uncertainties. Han *et al.* (2017) also obtain a moment tensor for our event 3 that has a double-couple source component with a strike to the northeast that is in agreement with the strike of our locations in Figure 2.

In this article, we interpret and identify these 14 events as one known cavity collapse near the 2017 explosion and 13 earthquakes several kilometers to the north by correlation data, the locations, polarities, and discriminant data. Our companion paper (Kim *et al.*, 2018) classifies all of these 13 events by an independent technique (P/S spectral ratios) to be earthquakes (though it required more than MDJ data to be confident for the first of the two aftershocks on 9 December 2017). The different identification methods agree with independent evidence that these are earthquakes so this is our favored explanation.

There was an initial disagreement between the two methods in the identification of event 8. The correlation data of Lg waves indicated that event 8 is part of the cluster with a high degree of confidence. The linear discriminant using P/S spectral ratios in Kim *et al.* (2018) initially identified event 8 as an explosion on the basis of data from MDJ. To resolve this discrepancy, we examined event 8 more closely. Event 8 is strongly connected to the cluster with 23 observations and 5 of the 12 other events. In fact, it was the template event used to detect the other events. For the station in question, MDJ, it is connected to four other events in the locations. Therefore, if 8 is part of the cluster of similar events, we argue that they are of the same event type, that has been identified as earthquakes for 12 of the events by two independent methods. The degree of confidence we have in this statement depends on the degree of similarity measured by CC, its statistical significance from the time–bandwidth product, the numbers of observations, the number of events, and the locations. The mean CC of event 8 equal to 0.39 is high and similar to the rest of events in the cluster (Ⓔ Table S2).

The CC of event 8 with event 9 is 0.77, which is the highest of the 23 observations and also occurs at station MDJ, which had the inconsistent results. A CC equal to 0.77 is extremely statistically significant for this time–bandwidth product, although we are not able to quantify it with a numeric value. If 8 is an explosion and 9 is an earthquake, then it is unlikely to (1) have an extremely high CC of 0.77 at station MDJ, (2) have it occur 26 min before, (3) have it occur 35 m away, and (4) have similar magnitudes (3.0 and 2.8, 0.2 units difference). These two events have the characteristics of triggered repeating events seen in China and California. To have had all of these things happen would require a very accurate earthquake prediction of the absolute location, origin time, and magnitude of a small earthquake to occur, with these extremely small separations from event 9. Even if the earthquake were able to be accurately predicted, it appears physically impossible to have event 8 be an explosion and event 9 be an earthquake and meet all these qualifications. The P/S spectral ratio data at MDJ appear to cause a misclassification of event 8, due to noise contaminating the record. But the Lg correlation data combined with high-precision locations correctly classify event 8 to be in the same population as the other 12 earthquakes for all the 23 observations, including the best at MDJ, which was the station in question.

The misclassification probability p of the linear discriminant without the benefit of the correlation data was 0.5% when considering events one-at-a-time. For a pair of events, such as 8 and 9 that are highly similar, the correlation data indicate they are the same event type that could be either both earthquakes or both explosions. The reason why we believe the cluster is all earthquakes is because the correlation data identify them as the same event type, and the discriminant results initially identified 12 of the 13 events to be earthquakes. For the discriminant analysis to incorrectly identify 12 events, the probabilities multiply, giving a misclassification probability of $p^{12} = 0.005^{12}$, which is near zero. Therefore, having a larger cluster of similar events not only allows a more unambiguous determination of event type but also gives much greater confidence in the statistical significance of that identification by reducing the misclassification probability from 0.5% for one

event to near zero for many events. This illustrates the combined strengths of the two complementary and independent methods for identifying events by the discriminant analysis and correlation data. For a more complete and detailed discussion of the probability analysis for various scenarios and assumptions, see the Ⓔ Estimating Confidence in the Statistical Significance of Identification section in the electronic supplement.

For the problem event 8, it appears that the signals are correlated and give the correct classification as an earthquake using the correlation data. But the noise is uncorrelated and gives a misclassification for event 8 at MDJ using the discriminant. The *Lg* waveforms are correlated at all stations and event pairs, including the problem station MDJ. This means that the sources are similar and that the signals for the *P* and *S* waves are also probably correlated at MDJ for event 8, but the noise is what causes an error. Actually, the seismograms in Kim *et al.* (2018) verifies this conclusion that there appears to be a noise burst at the same time as the *P*-wave arrival.

The 23 September **M** 3.3 event 3 was also initially misclassified. From Ⓔ Table S2, we see that this event is the most strongly connected to the cluster with the most observations, 29, the highest CC of 0.83, and the second highest mean CC of 0.49. From the same arguments as for event 8 above, we can determine with a high degree of confidence that this event is also an earthquake from the correlation and location data and discriminant data that identified it as an earthquake.

Used in isolation, the waveform similarity measured by cross correlation has no physical basis for identifying events. It is a relative event method, and its strength is in classifying events with a high degree of certainty to be of the same event type, which can be with known explosions or earthquakes, or verified by some independent means, such as the linear discriminant we use. However, the high-precision location data that are obtained from the differential travel times of correlation measurements can provide an independent identification with a physical basis, because we make the case here that the locations are more likely earthquakes on a fault than explosions. This identification as earthquakes can be further verified when focal mechanisms, a mapped fault trace on the surface, or lineaments in the topography are available that match the orientation of the fault determined by the locations.

CONCLUSIONS

We achieve precision at the level of about 70 m in relative location for 13 aftershocks of the 2017 nuclear explosion at the North Korea test site that appears to image a fault about 700 m long. In the direction of the best station coverage, a precision of 19 m is resolved. It is significant that such precision can be obtained using stations on average 410 km away, a factor of about 6000 difference in length scales (410/0.069). Our results are derived from the combined benefits of waveform cross correlation, double-difference relocation, and *Lg* being a slow wave. We also demonstrate significant improvement for correlation and location data to be used for identifying event type. Together, they provide complementary and independent evidence for the identification and characterization of seismic events, and, when combined with other methods, increase the statistical significance of those classifications substantially. In the case of these 13 aftershocks combining our discriminant data and correlation and location data, we identify the cluster to be all earthquakes, with a near-zero probability of misclassification. There is a 92% probability that the discriminant identification using MDJ data alone initially misclassified one event as an explosion, assuming the correlation data are correct, for which we have a high degree of confidence because of the high similarity of these events.

There are valid and understandable reasons for this discrepancy when examining the record for the one problem station MDJ that appears to have a noise burst at the *P*-wave arrival. Using discriminant data alone could cause a problem because this misclassification as an explosion occurred for a small event at the North Korean nuclear test site. This does not mean that the discriminant method is not a good technique in most cases. But any technique is limited by the quality of the data. It has a misclassification probability that is quite low by itself of 0.5%, and for a set of 13 events, it is not unexpected that one could be misclassified within that uncertainty. The combined power of the low misclassification probability of the discriminant method together with the high probability that all the events are in the same cluster of the same type from the correlation data gives us much greater confidence in the correct identification of all the events.

The good news is that the conclusions of this article have been verified by subsequent analysis in Kim *et al.* (2018), adding two more stations with better data that now correctly identify all 13 events as earthquakes, including event 8 that was initially identified as an explosion. The two methods now agree 100% in the identification of these 13 aftershocks, demonstrating the combined power of the complementary approaches and the greater statistical significance that results than that for either method by itself.

Correctly identifying small seismic events can be especially challenging and problematic as is shown by the 12 May 2010 problem event and the examples here with event 8, as well as the 23 September M 3.3 event 3 in the aftershocks of the 2017 explosion that some agencies initially misclassified. These three small seismic events were all of great concern because they occurred at the North Korean test site and were thought to be explosions by some groups using different methods and data. Now, it appears that all agencies, including our own work with correlation and location data and a linear discriminant, agree that these aftershocks of the 2017 nuclear test are not explosions.

DATA AND RESOURCES

Waveform data were obtained from International Monitoring System (IMS) stations USA0B and KS31 through vDEC (the Virtual Data Exploitation Centre of the Comprehensive Nuclear-Test-Ban Treaty Organization) via a special research contract; from the Korean Meteorological Agency by special

permission; and (for stations MDJ and INCN) from the Incorporated Research Institutions for Seismology (IRIS) Data Management Center (http://ds.iris.edu/SeismiQuery/) and from the U.S. National Data Center (USNDC) for the more recent IMS data. We also searched bulletins for phase picks and event locations, as reported by the International Seismological Centre at http://www.isc.ac.uk/iscbulletin/search/ and in the Advanced National Seismographic System Comprehensive Earthquake Catalog available at https://earthquake.usgs.gov/earthquakes/search/. Computations were performed and figures were created with MATLAB v.8.0.0.783, and some plots were created with the Generic Mapping Tools (GMT) package (Wessel and Smith, 1995). All websites were last accessed on August 2018.

ACKNOWLEDGMENTS

The authors thank staff at the International Data Centre (IDC), Comprehensive Nuclear-Test-Ban Treaty Organization (CTBTO) in Vienna, Austria, who kindly assisted us in acquiring waveform data from the IDC archive using the Virtual Data Exploitation Centre (vDEC). The authors thank Guest Editor Lianxing Wen, Steve Gibbons, and an anonymous reviewer for helpful comments on this article. Our work has been supported by the Consortium on Verification Technology under the Department of Energy/National Nuclear Security Administration Award DE-NA0002534 via a subcontract between Columbia University and the University of Michigan and by the Defense Threat Reduction Agency under Award HDTRA-1-11-1-00027. This is Lamont–Doherty Earth Observatory Contribution Number 8250.

REFERENCES

Adushkin, V. V., and A. A. Spivak (1995). Aftershocks of underground nuclear explosion, pp 35–49 in Earthquakes induced by underground nuclear explosions, *Proc. of the NATO Advanced Research Workshop*, Moscow, Russia, 9–12 November 1994, Springer-Verlag Berlin and Heidelberg GmbH & Co.

Chidambaran, R. (2000). Excerpt from the text of a forthcoming book Technology and Security: India's Long-term Interests), available at http://archive.is/4STUJ#selection-805.0-821.1009 (last accessed August 2018).

Console, R., and A. V. Nikolaev (1995). Editors of earthquakes induced by underground nuclear explosions, *Proc. of the NATO Advanced Research Workshop*, Moscow, Russia, 9–12 November 1994, Springer-Verlag Berlin and Heidelberg GmbH & Co.

De Geer, L.-E. (2012). Radionuclide evidence for low-yield nuclear testing in North Korea in April/May 2010, *Sci. Global Secur.* **20,** 1–29.

De Geer, L.-E. (2013). Reinforced evidence of a low-yield nuclear test in North Korea on 11 May 2010, *J. Radioanal. Nucl. Chem.* **298,** no. 3, 2075–2083, doi: 10.1007/s10967-013-2678-5.

Han, L., Z. Wu, C. Jiang, and J. Liu (2017). Properties of three seismic events in September 2017 in the northern Korean Peninsula from moment tensor inversion, available at https://arxiv.org/abs/1710.01586.

Kim, W.-Y., P. G. Richards, D. P. Schaff, E. Jo, and Y. Ryoo (2018). Identification of seismic events on and near the North Korean test site following the underground nuclear test explosion of 2017 September 3, *Seismol. Res. Lett.* doi: 10.1785/0220180133.

Kim, W.-Y., P. G. Richards, D. P. Schaff, and K. Koch (2017). Evaluation of a seismic event, 12 May 2010, in North Korea, *Bull. Seismol. Soc. Am.* **107,** no. 1, 1–21, doi: 10.1785/0120160111.

Klein, F. W. (2007). User's guide to HYPOINVERSE-2000, a Fortran program to solve for earthquake locations and magnitudes, *U.S. Geol. Surv. Open-File Rept. 02-171*, 121 pp.

Liu, J., L. Li, J. Zahradník, E. Sokos, C. Liu, and X Tian (2018). North Korea's 2017 test and its non-tectonic aftershock, *Geophys. Res. Lett.* **45,** no. 7, 3017–3025, doi: 10.1002/2018GL077095.

Richards, P. G., and G. Ekström (1995). Earthquake activity associated with underground nuclear explosions, in *Earthquakes Induced by Underground Nuclear Explosions*, *Proc. of the NATO Advanced Research Workshop*, Moscow, Russia, 9–12 November 1994, Springer-Verlag Berlin and Heidelberg GmbH & Co., 21–34.

Schaff, D. P., and P. G. Richards (2004). *Lg*-wave cross correlation and double difference location: Application to the 1999 Xiuyan, China, sequence, *Bull. Seismol. Soc. Am.* **94,** 867–879.

Schaff, D. P., and P. G. Richards (2011). On finding and using repeating seismic events in and near China, *J. Geophys. Res.* **116,** no. B03309, doi: 10.1029/2010JB007895.

Schaff, D. P., W.-Y. Kim, and P. G. Richards (2012). Seismological constraints on proposed low-yield nuclear testing in particular regions and time periods in the past, with comments on "Radionuclide evidence for low-yield nuclear testing in North Korea in April/May 2010" by Lars-Erik De Geer, *Sci. Global Secur.* **20,** 155–171, doi: 10.1080/08929882.2012.711183.

Schaff, D. P., P. G. Richards, M. Slinkard, S. Heck, and C. Young (2018). *Lg*-wave cross correlation and epicentral double-difference location in and near China, *Bull. Seismol. Soc. Am.* **108,** no. 3A, 1326–1345, doi: 10.1785/0120170137.

Tian, D., J. Yao, and L. Wen (2018). Collapse and earthquake swarm after North Korea's 3 September 2017 nuclear test, *Geophys. Res. Lett.* **45,** no. 9, 3976–3983, doi: 10.1029/2018GL077649.

Wessel, P., and W. H. F. Smith (1995). New version of the generic mapping tools released, *Eos Trans. AGU* **76,** no. 33, 329, doi: 10.1029/98eo00426.

Wright, C. M. (2013). Low-yield nuclear testing by North Korea in May 2010: Assessing the evidence with atmospheric transport models and xenon activity calculations, *Sci. Global Secur.* **21,** 3–52.

Zhang, M., and L. Wen (2015). Seismological evidence for a low-yield nuclear test on 12 May 2010 in North Korea, *Seismol. Res. Lett.* **86,** no. 1, 1–8, doi: 10.1785/02201401170.

David P. Schaff
Won-Young Kim
Paul G. Richards
Lamont-Doherty Earth Observatory
Columbia University
61 Route 9W
Palisades, New York 10964 U.S.A.
dschaff@LDEO.columbia.edu

Eunyoung Jo
Yonggyu Ryoo
Earthquake and Volcano Monitoring Division
Korea Meteorological Administration
61, 16-gil Yeouidaebang-ro, Dongjak-gu
Seoul 156-720
Republic of Korea

Published Online 19 September 2018